91-21

R. Taranko*

QUASIPARTICLE ELECTRONIC STRUCTURE
OF THE DEGENERATE HUBBARD MODEL

――――――――――――
* On leave of absence from Institute of Physics,
M.Curie-Sklodowska University,
20-031, Lublin, Poland

1991

1. Introduction

It is well known that the photoemission experiments on the d-band transition metals deviate from the results of the band structure calculations. Especially nickel is an example for which discrepancies are very serious. For example, the measured d-band width is smaller by about 30% than the calculated one[1-3], a resonant satellite structure appears on the quasiparticle band structure about 6 eV below the Fermi level[4,5] and the exchange splitting near the top of the fifth d-subband is only half as large as the predicted from band theory[1,6-8].

Now it is generally accepted that these effects can be understood as consequences of strong correlations in the Ni d-bands.

A realistic model to describe such electron correlations in narrow energy bands was proposed by Hubbard[9], and in the simplest case the Hamiltonian takes form

$$H = \sum_{ij\sigma} t_{ij} a_{i\sigma}^+ a_{j\sigma} + U/2 \sum_{i\sigma} n_{i\sigma} n_{i-\sigma} \qquad (1)$$

where the creation (annihilation) operators for electrons in Wan - nier states associated with the i-th site index with σ are given by $a_{i\sigma}^+ (a_{i\sigma})$. The operator $n_{i\sigma}$ is the corresponding number operator and U characterizes the strength of the intra-atomic Coulomb interaction.

The electron correlation effects can be allowed for by introducing the self-energy $\sum(\vec{k}, E)$. The real part of this function corresponds to the shifted energy eigenvalues and the imaginary part implies broadening of the bands. Once we have it, we can calculate the one-electron spectral function

$$A(\vec{k}, E) = -\frac{1}{\pi} Jm \left(E^* - \epsilon_{\vec{k}} - \sum(\vec{k}, E^*) \right)^{-1}. \qquad (2)$$

Without the many-body interactions the spectral function (2) reduces to a set of delta functions peaked at the corresponding band energies. Due to many-body interactions, the spectral function will be extended over a wide energy range and will show more or less pronounced structure. In recent years, there has been a considerable amount of experimental work dealing with the metal electronic band structure. The experimental band structure determined, e.g. from photoemission data corresponds for every $\vec{k}$-value to the maxima of the spectral function

(2). In this context, it is evident that the self-energy $\Sigma(\vec{k}, E)$ is a very important characteristic of the many-electron system and its careful calculation is very desirable.

Since the three-dimensional Hubbard model is not integrable, there are different approximate methods for including the correlation effects. In spite of many attempts which seemed to be very reasonable[10-14] we have decided to calculate the self-energy within second-order in U/W (W being the bandwidth) perturbation approach[15-23]. Although the perturbation series expansion has not had its convergence properties investigated and it may be convergent for small values of the parameter U/W or the convergence may only be asymptotic, it is also (especially in recent years) widely used in investigations of the heavy fermion problem described by the Periodic Anderson Model (PAM)[24-28]. This method of description of the correlation effects automatically reproduces the Fermi liquid behaviour which is usually expected to be fulfilled[29]. Most of the existing approximations have difficulties in reproducing properly this Fermi liquid behaviour[27] (for PAM).

Recently, Bulk and Jelitto[17] have performed the calculations of the quasiparticle band structure using the one-band Hubbard model. The correlation effects were included within the modified second-order perturbation theory intended to describe also stronger correlations than one usually tries to describe within the standard second-order perturbation approach. In addition, the calculations were performed in a self-consistent way, although only the quasiparticle occupation numbers and the chemical potential were calculated in a selfconsistent scheme. It means that the quasiparticle band structure needed for the calculation of the self-energy was unchanged during the selfconsistency process. Also, the self-energy they used depends on a wave vector only through the first $\vec{k}$-dependent term in a special expansion formula. As we have shown in Ref.[30], such a short expansion formula can give for the self-energy in some cases results which are even worse than the obtained within so-called local approximation ($\vec{k}$-dependence of the self-energy is retained absolutely).

The purpose of this work is to investigate the quasiparticle band structure based on a more realistic version of the Hubbard model (1), namely, on the degenerate d-band model. We also present the self-energy curves with full $\vec{k}$-dependence as well as we use this nearly exactly calculated self-energy for calculations of the spectral density of the quasiparticle states, quasiparticle energy bands and quasiparticle density of states. We have performed all these calculations within non-self-consistent and selfconsistent ways. In the case of selfconsistent approach we have used at each next step of the iteration process the ener-

gy band structure obtained in the preceding step.

The paper is organized as follows. In the next section we present the results of the $\vec{k}$ –dependent self-energy calculations. In Sec. 3, we give the spectral density of states, the quasiparticle energy bands and the quasiparticle density of states calculated within the non-self-consistent approach and in Sec. 4 within the selfconsistent approach. Sec. 4 contains also some remarks and conclusions.

2. The second-order U –perturbation self-energy

For the sake of completeness we shall briefly outline the main ideas used in computation of the second-order contribution to the self-energy. We refer to our previous paper for more details[30], see also for independent similar calculations performed for PAM in[26].

The second-order contribution to the self-energy for electrons in d-band degenerate Hubbard model reads (we consider a paramagnetic case and the spin indices will be omitted):

$$M(\vec{k},E)= \frac{9U^2}{N^2} \sum_{\vec{p}\vec{q}} \frac{f_{\vec{q}}(1-f_{\vec{k}+\vec{p}})(1-f_{\vec{q}+\vec{p}}) + (1-f_{\vec{q}}) f_{\vec{k}+\vec{p}} f_{\vec{q}+\vec{p}}}{E + \epsilon_{\vec{q}} - \epsilon_{\vec{k}+\vec{p}} - \epsilon_{\vec{q}+\vec{p}}} \ . \tag{2}$$

The numerical factor 9 corresponds to all the available scattering channels for a given spin electron. Now U is the average on-site Coulomb integral taken to be the same for each of the five d-bands.

The expression for the self-energy (2) can be arranged in the form ([15-17,20,25-28,30])

$$M(\vec{k},E)=9U^2 \sum_{\vec{R}} e^{i\vec{k}\cdot\vec{R}} \int\!\!\!\int\!\!\!\int_{-\infty}^{+\infty} \frac{d\omega_1\,d\omega_2\,d\omega_3}{E+\omega_1-\omega_2-\omega_3} N(\omega_1,\omega_2,\omega_3) D(\vec{R},\omega_1) D(\vec{R},\omega_2) D(\vec{R},\omega_3)$$

$$\equiv 9U^2 \sum_{\vec{R}} e^{i\vec{k}\cdot\vec{R}} M(\vec{R},E) \tag{3}$$

where the function $N(\omega_1,\omega_2,\omega_3)$ contains all $f_{\vec{k}}$ factors appearing in Eq. (2) and $\vec{R}$ denotes atomic positions in the crystal. The functions $D(\vec{R},E)$ are "the lattice density of states" corresponding to the lattice Green functions[31,32]:

$$G(\vec{R},E)=\frac{1}{N} \sum_{\vec{k}} e^{i\vec{k}\cdot\vec{R}} (E-\epsilon_{\vec{k}})^{-1}. \tag{4}$$

Note that in formula (2) as well as in formula (3) we have to do six-fold integration. This rather inconvenient, from computational point of view, formulas can be transformed as follows[17,26,30]:

$$M(\vec{k},E) = 9U^2 \sum_{s=0}^{\infty} \epsilon(R^s,\vec{k}) M(\vec{R}^s,E) \tag{5}$$

4

where $\epsilon(R^s,\vec{k})=\sum_{\vec{R}}^{|\vec{R}|=R^s} e^{i\vec{k}\cdot\vec{R}}$; $\epsilon(R^\circ,\vec{k})=1$, $R^s=|\vec{R}|$,

$$D(R^\circ,E)=D^{FE}(E)$$

and $D^{FE}(E)$ corresponds to the band structure $\epsilon_{\vec{k}}$. Here $\vec{R}^s$ denotes the position vector of the atoms lying in the same neighbour shell and the sum is performed over neighbour shells. Such a reformulation of the initial expansion formula for $M(\vec{k},E)$ is possible because "the lattice density of states" $D(R^s,E)$ is the same for all vectors $\vec{R}^s$ connecting the central atom with atoms lying at the same distance from it (here "s" enumerates the successive neighbour shells). The functions $\epsilon(R^s,\vec{k})$ for successive values of s have been given in Ref. /30/. In this way, in order to obtain the self-energy at many $\vec{k}$ -points of the Brillouin zone (BZ), one has to calculate the 3-fold integrals at the beginning of the problem and multiply them by functions $\epsilon(R^s,\vec{k})$. All $\vec{k}$-dependence of the self-energy is contained in the functions $\epsilon(R^s,\vec{k})$ and energy-dependence in the 3-fold integrals. The first term in expansion (5) corresponds to the local approximation of Treglia et al/15/ and the first two terms correspond to the formula used by Bulk and Jelitto in investigations of the one-band Hubbard model/17/. Note that in order to perform self-consistent calculations, one should begin working with the self-energy expressed in the general form

$$M(\vec{k},i\omega_m)=-9\left(\frac{UT}{N}\right)^2\sum_{\omega_1,\omega_2,\vec{p},\vec{q}} G_{\vec{k}+\vec{q}}(i\omega_1)G_{\vec{p}-\vec{q}}(i\omega_m+i\omega_2-i\omega_1)G_{\vec{p}}(i\omega_2)$$

rather than in the form (2). Here, T denotes the temperature and $i\omega_m$ the Matsubara frequencies. All further calculations remain the same except for $D(R^s,E)$ to be inserted

$$D(R^s,E)=-\frac{1}{\pi}\,\Im m\,\frac{1}{N}\sum_{\vec{k}} G_{\vec{k}}(E)e^{i\vec{k}\cdot\vec{R}^s} \tag{6}$$

This idea was used by Schweitzer and Czycholl in second-order U -perturbation treatment around the nonmagnetic Hartree-Fock solution of PAM /27/. They gave also another efficient algorithm for computations of the 3-fold integrals appearing in Eq. (5). Note that usually one calculates the imaginary part of the self-energy and this means one has to perform two-dimensional integrals over some appropriate area in the energy space /33/. Instead of this procedure, Schweitzer and Czycholl transformed the 3-fold integral present in (5) to the following form:

$$-i\int_0^\infty d\lambda\, e^{i\lambda E}\left(A_{\vec{R}}^2(\lambda)B_{\vec{R}}(-\lambda)+A_{\vec{R}}(-\lambda)B_{\vec{R}}^2(\lambda)\right) \tag{7}$$
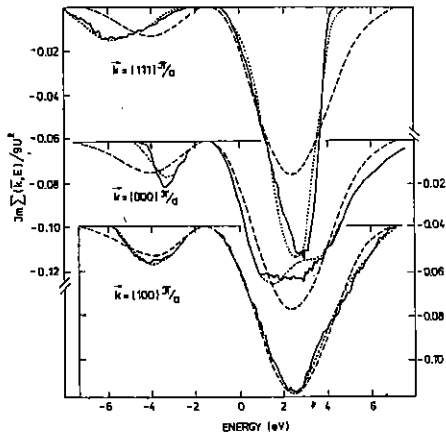
5

Fig. 1.

The imaginary part of the self-
-energy for N_e =1.25 el./bands.
The full lines - Monte-Carlo integ-
ration results, broken lines - lo-
cal approximation, dotted lines -
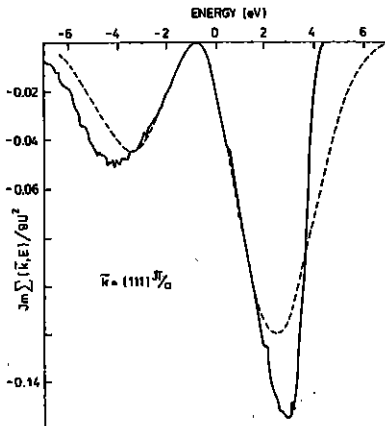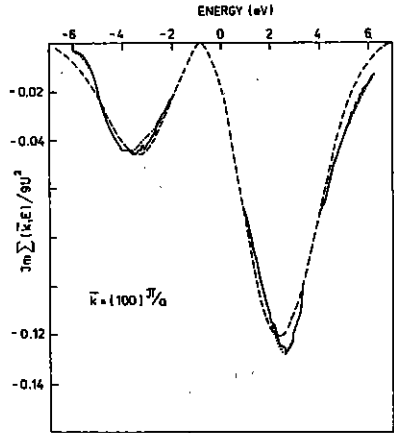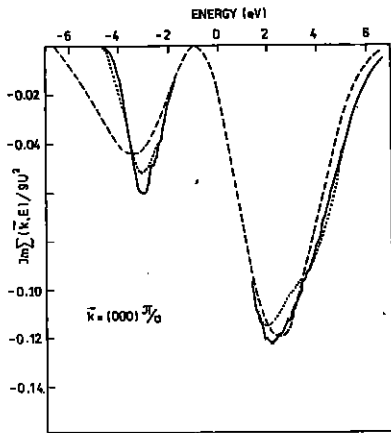calculations according to Eq.(5).

Fig. 2.

The imaginary part of the self-
-energy for N_e =2.5 el./bands.

where
$$A_{\vec{R}}(\lambda) = \int_0^\infty d\eta \, D(R,\eta) \, f(\eta) e^{-i\lambda\eta},$$
$$B_{\vec{R}}(\lambda) = \int_0^\infty d\eta \, D(R,\eta)(1-f(\eta)) e^{-i\lambda\eta},$$

and $Im \, E > 0$, $D(R,E)$ is given by Eq.(6). This way of calculations is very useful especially in the nonzero temperature case.

3. Self-energy, spectral density and quasiparticle density of states: non-selfconsistent results.

Let us apply the results of the previous section, Eqs. (2-4), for the calculations of the self-energy for a model electron band structure. Here, we compare the self-energy curves calculated within the commonly used local approximation with those calculated with full $\vec{k}$-dependence. In addition, we calculate the self-energy along formula (2) using the Monte-Carlo integration method. The double $(\vec{p}, \vec{q})$ sum in Eq. (2) was performed using for each $\vec{k}$-vector about one million of random generated pairs of vectors $(\vec{p}, \vec{q})$. First, we calculated the imaginary part and in the next step, the real part by the Kramers-Kronig relation. The calculations here done for a model SC crystal lattice with degenerate electron energy bands $\epsilon_{\vec{k}}$ calculated in a tight-binding scheme for s-wave funtions with nearest-neighbour hopping integrals, only. The bandwidth W equals 6 eV and the band limits are (-3eV, 3eV). We have checked that formula (5) with the first six terms included works very well and such expansion can be served as a fast method (in comparison with the Monte-Carlo type integration) for the self-energy calculations. Here, we give extensive numerical results for various bandfillings, Figs. 1-5. The full curves denote the results of Monte-Carlo type integrations, the broken curves represent the results obtained within local approximation (only the first term in Eq.(5) is taken into account) and the dotted curves show the results obtained by using Eq.(5) with the first six terms included. In all these figures we give only the imaginary part of the self-energy. In Figs. 1-4 and 5 the bandfilling is equal to N_e =1.25, 2.50, 5.0, 7.5 and 8.75 electrons/bands, respectively. For all cases we show the results for three values of the $\vec{k}$-vector, namely for $\vec{k}$=(000)π/a — Γ, $\vec{k}$ = (100)π/a — X, $\vec{k}$ = (111)π/a — R. At the first sight, we can conclude that the $\vec{k}$-dependence of the self-energy is most prominent at the point Γ of BZ. At this point of $\vec{k}$-space there are largest differences between the local approximation and exact calculations. They can be explained by looking at the formula (5) (cf. /17/). The successive terms in this expansion formula enter into the general expression for the self-energy with "weights"
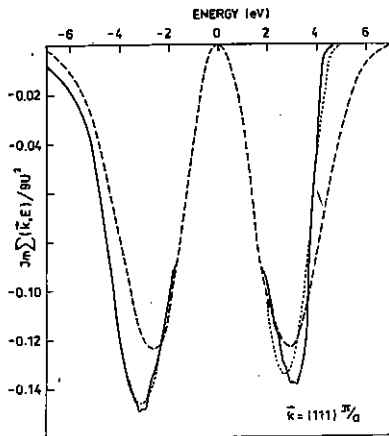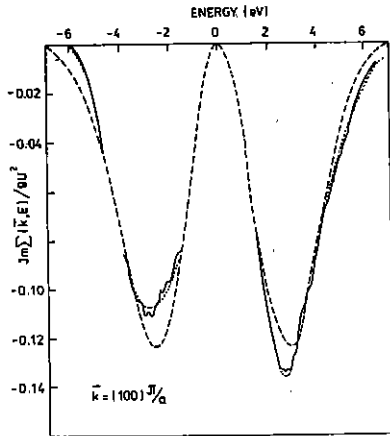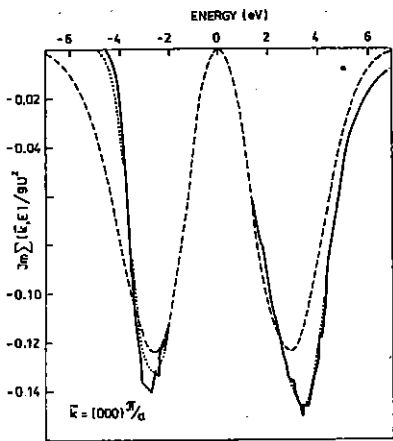
Fig. 3.
The imaginary part of the self-energy
for N_e = 5 el/bands.

equal to 1, 6, 12, 8, 6, 24 for point
Γ ; and for example for point X ,
with "weights" equal to 1,2,0,-8,6,8,
respectively. Note that our 6-terms
expansion is sufficiently good in com-
parison with the exact results. On
the other hand, the local approximation
seems to be rather unsatisfactory, es-
pecially for bandfillings far away from
the half-filled case - see, e.g. N_e=
2.5 el./bands, point Γ for $E < E_F$
and point R for $E > E_F$; N_e =1.25 el./bands, point R for $E < E_F$,as
well as, for $E > E_F$; N_e =7.5el./bands, point Γ for $E < E_F$; N_e =8.75
el./bands, point Γ for $E < E_F$. So large discrepancies between the
exact results and the obtained within local approximation may lead, as
rule, to different lifetimes and energies of the corresponding quasi-
particles. For example, there are especially great differences in the
values of the imaginary part of the self-energy for $\vec{k} = (000)\Pi/a$, N_e=
8.75 el./bands, Fig. 5. The main (exact) minimum is about 40% deeper
than the one obtained within the local approximation, and there is a
low energy tail only within the local approximation.
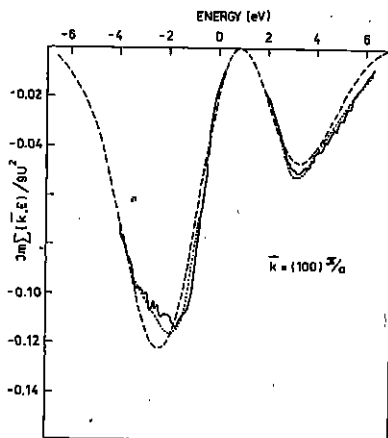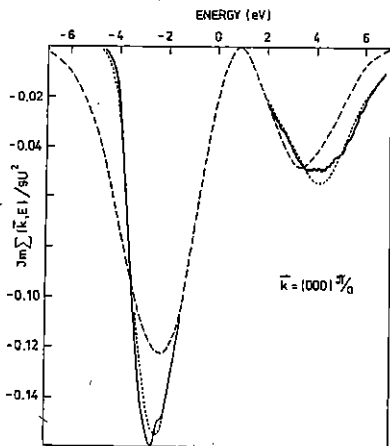   It is interesting to study to what extent these differences in

8

Fig. 4.

The imaginary part of the self-
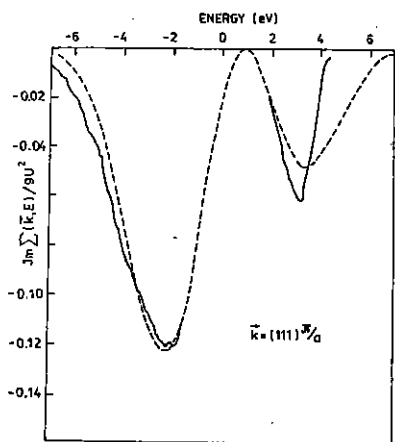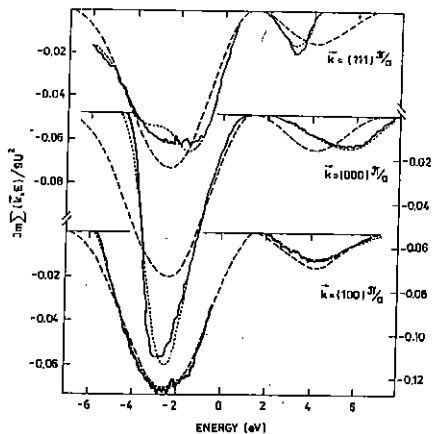-energy for N_e =7.5 el./bands.

Fig. 5.

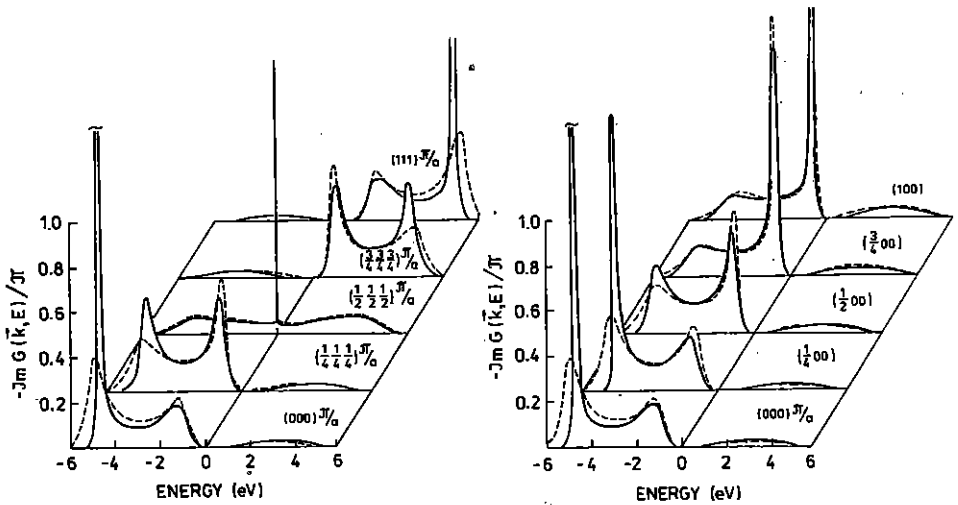The imaginary part of the self-
-energy for N_e =8.75 el./bands.

9

Fig. 6.
The spectral density of states for N_e =5 el./bands and U/W =1/4.
The full (broken) lines correspond to the self-energy calculated
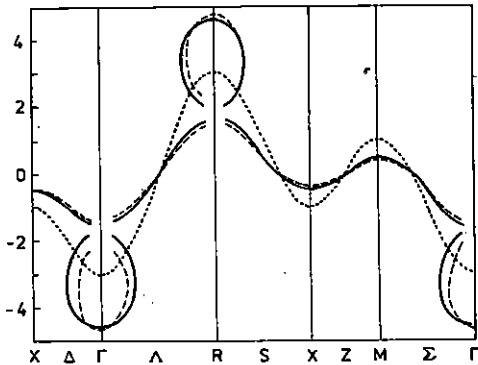according to Eq.(5) (local approximation).

Fig. 7.
The quasiparticle band structure along
different directions of SCC BZ for
N_e =5 el./bands and U/W =1/4. The full
(broken) lines correspond to the self-
-energy calculated according to Eq.(5)
(local approximation). The dotted line
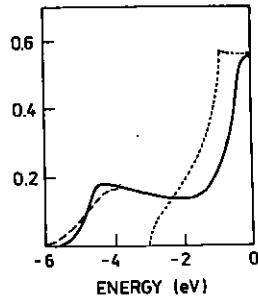represents the Hartree-Fock solution.

Fig. 8.
The quasiparticle density
of states for the case desc-
ribed in Fig. 7.

10

the self-energy curves can modify the spectral density of states, or equivalently, can lead to changes of the energy and lifetimes of the corresponding quasiparticles. Therefore, we have calculated the spectral density of states, $-\frac{1}{\pi} \, \mathfrak{Im} \, (\, E - \epsilon_{\vec{k}} - \Sigma(\vec{k}, E))^{-1}$, for the band-fillings N_e =5 el./bands and N_e =8.75 el./bands for two values of the Coulomb strength U/W=1/4 and U/W=1/2, Figs. 6,9 and 12,15, respectively. In these figures we have displayed the spectral density of states for two special directions in BZ, namely for $\Gamma-X$ and $\Gamma-R$ directions. Looking at Figs. 6,9,12 and 15 one can observe the existence of two groups of well defined peaks in the spectral density of states. One group of peaks is centered essentially around the point Γ (R) the low (high) -energy excitations, and the second group is spread over the whole BZ. The comparison of the solid and broken curves emphasizes the necessity of including the full $\vec{k}$-dependence into the self-energy. We observe expressive effect on the lifetime of the excitations which we identify with the narrow peaks in the spectral density of states. In comparison with the results of Ref.$/30/$ in which only first two terms in formula (5) are used, we observe significant quantitative changes within the low- and high-energy excitations. The lifetimes of the corresponding quasiparticles increased significantly. On the other hand, the influence of the self-energy $\vec{k}$-dependence on the quasiparticles extending over whole BZ is rather small and leads to decreasing of their lifetimes. The increasing of the lifetime of the low- and high-energy quasiparticles can be simply explained in terms of the $\vec{k}$- and E-dependence of the self--energy, see Figs. 3-4. Just taking into consideration the full $\vec{k}$-dependency of the self-energy leads to the disappearance of its long low-energy tail (for point Γ at $E < E_F$ and small bandfillings) or high--energy tail (for point R at $E > E_F$ and large bandfillings). This means that the corresponding quasiparticles are nearly not damped in comparison with quasiparticles obtained within the local approximation. As for the peaks of the quasiparticle spectral density of states which belong to the energy band branch spreading over the whole BZ, one can observe the following effect due to the full $\vec{k}$-dependent self-energy. For half-filled bands the lifetime of these quasiparticle excitations is shorter independently of the correlation strength and for large band-fillings the lifetime of these excitations is longer.

For better understanding of the spectral density of states picture in our model system we have depicted in Figs. 7,10, and 13, 16 the solutions $E(\vec{k})$ of the equation

$$E(\vec{k}) - \epsilon_{\vec{k}} - \tfrac{9}{10} N_e U - M(\vec{k}, E(\vec{k})) = 0 \ . \qquad (8)$$

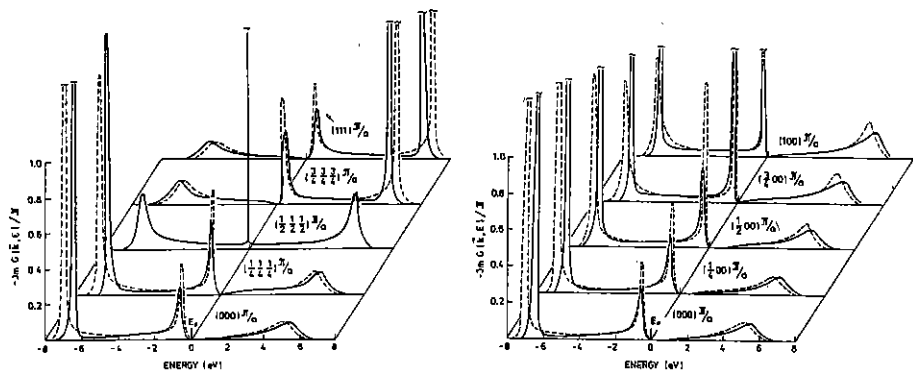Some of these solutions just represent the quasiparticle energy bands.

11

Fig. 9
The same as in Fig. 6 but for U/W =1/2.

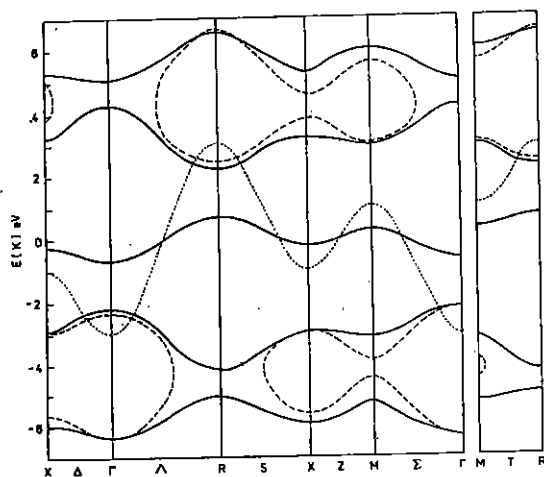
Fig. 10.
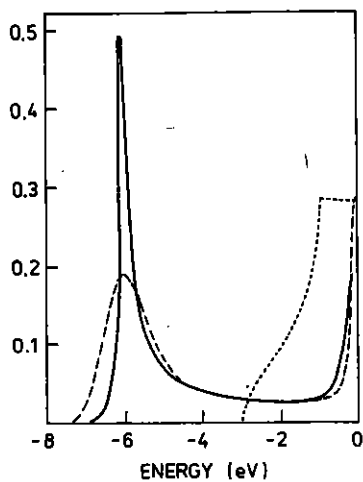The same as in Fig. 7 but for U/W =1/2.
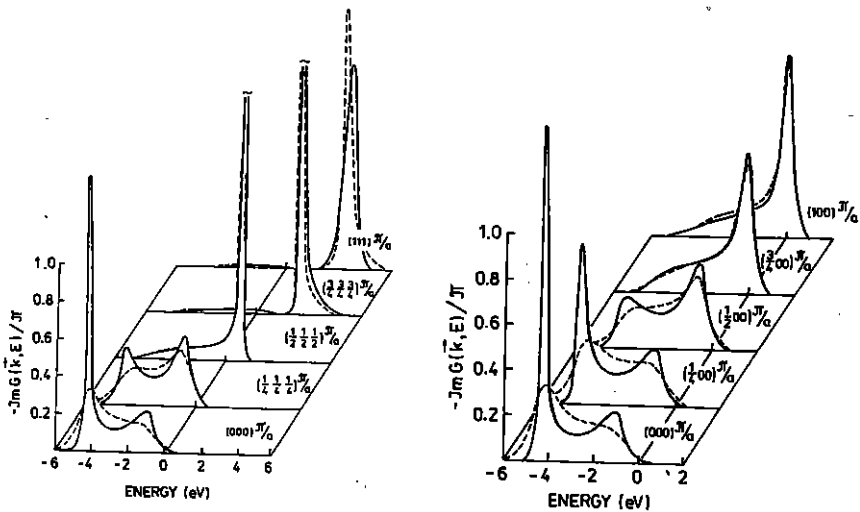
Fig. 11.
The same as in Fig. 8
but for U/W =1/2.

12

Fig. 12.

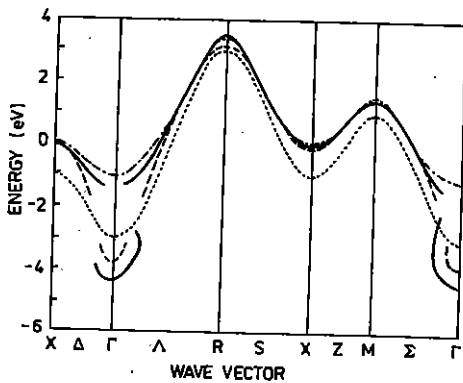The same as in Fig. 6 but for N_e =8.75 el./bands and U/W =1/4.

Fig. 13.

The same as in Fig. 7 but for N_e =8.75 el./bands and U/W =1/4. The broken-dotted line corresponds to the spectral density of states peak positions.
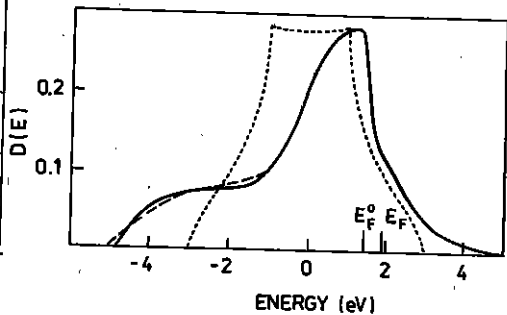
Fig. 14.

The same as in Fig. 8 but for N_e = =8.75 el./bands and U/W =1/4.

But one has to be careful because some of these $E(\vec{k})$ curves are merely mathematical solutions of Eq.(8) and do not represent any real physical quasiparticle band. Significance of such simultaneously performed calculations of the spectral density of states and solutions of Eq. (8) was thoroughly explained in Ref.[17] by Bulk and Jelitto. Here, we have also performed similar analysis but for degenerate d-band Hubbard model with nearly exact $\vec{k}$-dependent self-energy - Eq. (5). In Fig. 7 we present the solutions of Eq.(8) for the halffilled band case for $U/W = 1/4$. The dotted, full and broken curves correspond to the self-energy calculated within the Hartree-Fock approximation, exact and local approximation, respectively. We have depicted all mathematical solutions of Eq.(8), although, as we have mentioned above, some of them have no physical meaning. It is obvious that the figure has to be analyzed only simultaneously with the spectral density of state curves, Fig. 6. Then, it is clear that nearly circular in shape branch of solutions $E(\vec{k})$ in Fig. 7 which are located around Γ and R points of BZ do not correspond to the quasiparticle energy band. They correspond, speaking in the language of the spectral density of states, to the low-energy lying quasiparticle peaks located just mainly around Γ and R points of BZ. It should be also noted that only a lower (higher) part of these solutions correspond to the well defined peaks. The other part of this solution branch is situated in an energy region with large damping-compare the imaginary part of the self-energy in Fig. 3 for Γ (R) point for low (high) energies.

In Fig. 10 we present all solutions of Eq.(8) for the halffilled band but for stronger correlations, $U/W = 1/2$. At the first sight, one can notice five solution branches spreading over the whole BZ for the case of exact self-energy and only one branch for the case of approximate $\vec{k}$-independent self-energy (it is a middle one centered around zero energy value). But only after a careful comparison with the spectral density of states, Fig. 9, we can conclude that in this case there is only one quasiparticle energy band with the well defined peaks (of the corresponding spectral density) in the whole BZ with energies lying in a narrow energy region centered around zero energy value. Although one can observe very sharp peaks of the spectral density of states along a lowest branch of solutions of Eq.(8) for $\vec{k}$-points along Δ line of BZ, the corresponding peaks around R point of BZ are rather indistinctive from the broad background. For that reason we should not rather identify these branches of $E(\vec{k})$ with the quasiparticle energy bands. Two others branches of solutions of Eq.(8) are situated in an energy region corresponding to a large damping. Note that in the case of $\vec{k}$-independent
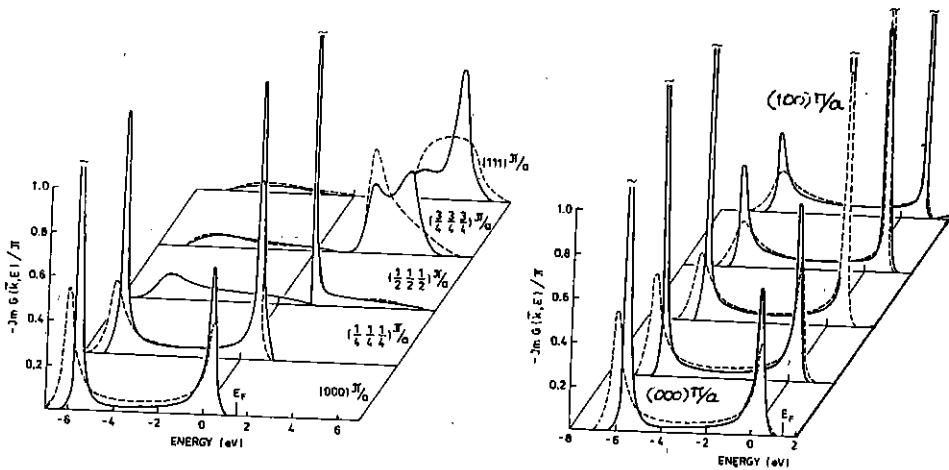
Fig. 15.
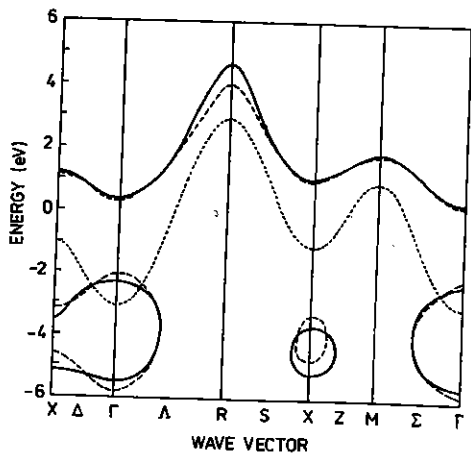The same as in Fig. 12 but for $U/W = 1/2$.

Fig. 16.
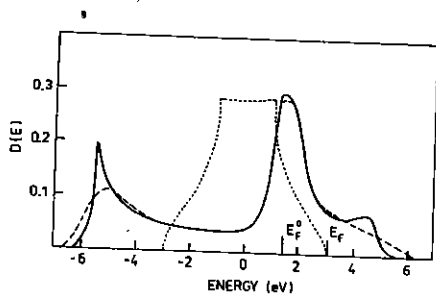The same as in Fig. 13 but for
$U/W = 1/2$.

Fig. 17.
The same as in Fig. 14 but for
$U/W = 1/2$.

15

self-energy there is only one branch of solutions of Eq.(8) in spite of small differences between heights of the quasiparticle peaks (full and broken curves).

In the case of nearly filled energy bands there is only one branch of solutions of Eq.(8) independently of the correlation strength, Figs. 13,16. The full $\vec{k}$-dependence of the self-energy leads to much better defined peaks of the spectral density especially for low-energy lying quasiparticle excitations.

The knowledge of the spectral density of states enables us to calculate the density of quasiparticle states

$$D(E) = -\frac{1}{N\pi} \sum_{\vec{k}} \Im \left(E^+ - \epsilon_{\vec{k}} - \sum (\vec{k}, E^+) \right)^{-1}. \tag{9}$$

In Figs. 8,11 we have displayed $D(E)$ for halffilled energy bands for U/W=1/4 and 1/2, respectively. Figs. 14 and 17 show the same function for nearly filled bands, N_e =8.75 el./bands. First of all we observe the satellite structures, especially clearly visible for stronger correlations independently of the bandfilling. They are very strong for half--filled bands and occur at the wings of the original energy band. In addition, we observe a pronounced narrowing of the central peak of the quasiparticle density of states. Comparing Figs. 7 with 8 and 10 with 11 one can attribute the narrow central peaks to the main branches of the quasiparticle band structure located on the energy scale in the vicinity of the zero energy value. The satellite structure can be explained by additional excitations visible on the spectral density of states, Figs. 6 and 4, and located around Γ and R points of BZ. The full $\vec{k}$-dependence of the self-energy influences, in principle, only the satellite regions of $D(E)$. It makes the satellite structures sharper and narrower. Note also a considerable band narrowing with increasing of the correlation strength. The quasiparticle density of states can be decomposed into three (two) parts for half-filled (nearly full) bands and the width of the main part of $D(E)$ can be attributed to the quasiparticle energy band, Figs. 7 and 8, 10 and 11, 13 and 14, 16 and 17.

In Figs. 14 and 17 we have marked on the energy axis the positions of the Fermi levels E_F^o and E_F ; E_F^o corresponds to the initial Hartree-Fock density of states (dropped lines) and is consistent with the corresponding bandfilling. The Fermi level E_F , on the other hand, is obtained using the quasiparticle density of states corrected by the correlation effects (solid line). It is clear that these differences between both values of the Fermi levels are consequences of the non-self-consistent calculations. In the case of the half-filled bands the Fermi levels E_F^o and E_F are the same for symmetry reasons.

4. The self-consistent approach

The non-selfconsistent U-perturbation treatment of the correlation effects in the Hubbard, PAM or Anderson models is very often used in literature in context of various problems (see for example [15,16, 18-20,24-27,30,33,34]). The non-selfconsistency means, however, that the quasiparticle band structure used for the calculations is not consistent with the one obtained from such calculations. Moreover, the Fermi level E_F calculated on the basis of the quasiparticle band structure is not equal to the one-electron Fermi level E_F^o. Due to the positive real part of the self-energy near E_F, the Fermi energy E_F is less negative than E_F^o (compare Figs. 14, 17). For that reason, some of the quasiparticles below the true Fermi energy E_F have infinite lifetimes and those at E_F have short lifetimes [19]. The first attempts to restore this deficiency of the non-selfconsistency was made by Kleinman and Mednick [19] but their procedure is not uniquely determined.

The idea of the selfconsistency in solid state physics is not new. We remind only here the theory of localisation of Götze [35], theory of superconductivity [36] or even the so-called Hubbard-III solution. Recently, we have performed the selfconsistent calculations of the quasiparticle density of states for the Hubbard model [22,23,33]. The main result of these calculations was the disappearing of the satellite structure on the quasiparticle density of state curves. These results were confirmed by other authors [28,37].

In order to compare the results of the previous sections with the selfconsistent calculations, we present here the spectral density of states, the quasiparticle energy bands (solutions of Eq.(8)) and quasiparticle density of states for N_e =5 el./bands and U/W =1/4, 3/8 (Figs. 18-20) and for N_e =8.75 el./bands, U/W =1/4, 1/2 (Figs. 21-22). We have performed calculations for half-filled bands and for U/W=3/8 (and not for U/W=1/2 as in Fig. 9-11) because of the numerical convergence problems. We hope that such a small difference in a correlation strength does not forbid us to make a comparison with the non-selfconsistent results obtained for U/W=1/2. The calculations were performed for the SC tight-binding electronic structure and all energies were measured in the half-bandwidth units (the initial free electron energy band was placed in (-1,+1) limits). The self-consistent procedure has been described in our papers [22,23]. The self-energy we have used in this approach was calculated within the local approximation. In this way, we can calculate the quasiparticle density of states performing only one-dimensional integrals at each step of the iteration process. On the contrary, using the full $\vec{k}$-dependent self-energy, one has to perform three-dimensional
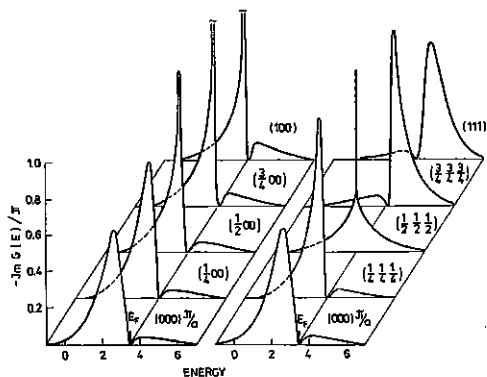
Fig. 18.

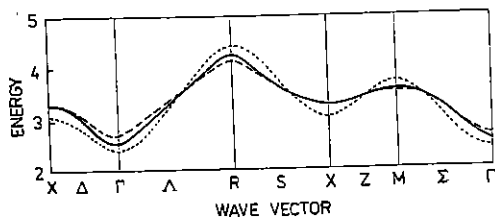The spectral density of states in selfconsistent approach. N_e =5 el./bands and U/W =3/8.

Fig. 19.

The quasiparticle band structure in a selfconsistent approach. N_e =5 el./bands and U/W =3/8. The full line corresponds to solutions of Eq.(5), the broken line corresponds to the spectral density of states peak's positions and dotted line corresponds to the Hartree-Fock solution.
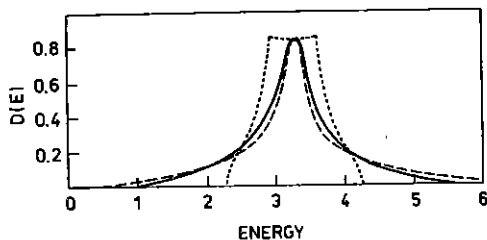

Fig. 20.

The quasiparticle density of states for N_e =5el./bands and U/W=1/4 (full line), U/W =3/8 (broken line). The dotted line represents the Hartree-Fock solution.
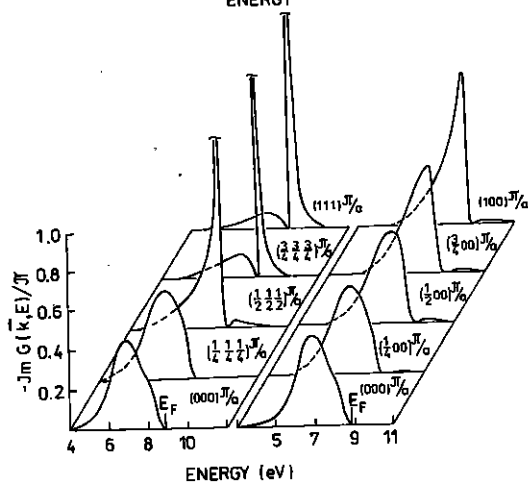
Fig. 21.

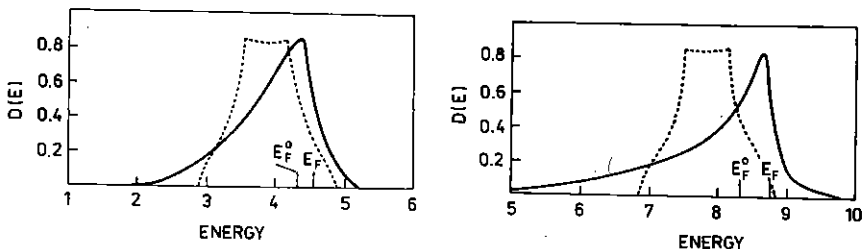The same as in Fig. 18 but for N_e =8.75 el./bands and U/W =1/2.

18

Fig. 22

The quasiparticle density of states in a selfconsistent approach for N_e =8.75 el./bands, U/W =1/4 (left-hand side) and U/W =1/2 (right-hand side).
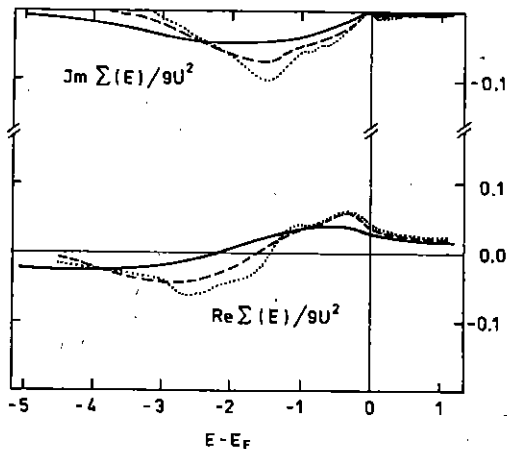

Fig. 23

The self-energy for nickel un-correlated density of states. The full (broken) line corresponds to U/W =1/4 (1/2) in a selfconsistent approach and dotted line in a non-selfconsistent approach.
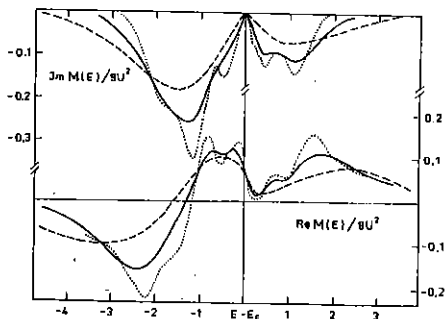

Fig. 24

The same as in Fig. 23 but for bcc canonical uncorrelated density of states with band-filling corresponding for iron.

integrals over a complex function for many energy values forming a suffi-
ciently dense energy grid. The knowledge of the quasiparticle density
of states on a dense energy grid is required because this function is
input data for the self-energy calculations. The replacement of the $\vec{k}$-
dependent self-energy by the $\vec{k}$-independent one can only be justified if
we could guarantee that such simplification does not introduce any qua-
litative changes in a final result. According to our earlier calcula-
tions, we can conclude that the selfconsistency process always removes
the satellite structure independently of its strength. Therefore, we ho-
pe that despite a stronger satellite structure in the case of $\vec{k}$-inde-
pendent self-energy, the selfconsistency process removes this structure
from the quasiparticle density of states, too.

As selfconsistent results for the quasiparticle density of states
do not exhibit any additional satellite structure, the quasiparticle
energy band should contain only one branch of values $E(\vec{k})$ without any
other possibilities. Indeed, in Fig. 19, N_e =5 el./bands, U/W =3/8, there
is only one band (full line). The dotted curve corresponds to the Hart-
ree-Fock result, and the broken curve was constructed using the energy
values corresponding to the positions of the spectral density of state
peaks. The spectral density of states, Fig. 18, contains for every $\vec{k}$-
value only one well obtained, sharp peak. There are many additional qua-
siparticle excitations at low energies (for Γ point of BZ) or at high
energies (for R point of BZ). The quasiparticle density of states cur-
ves, Fig. 20 - full (broken) line corresponds to U/W =3/8 (U/W =1/4), are
very smooth in comparison with those in Figs. 8,11. Very similar results
are obtained also for greater bandfillings. For example. Figs. 21 and 22
show the spectral density of states and the quasiparticle density of sta-
tes, respectively, for N_e =8.75 el./bands and U/W =1/2 - Figs. 21,22 left-
-hand side and for U/W =1/4 - Fig. 22 right-hand side.

In Figs. 23 and 24 we show the self-energy calculated within the
local approximation (dotted curves) in a non-selfconsistent way and in
a selfconsistent way. Fig. 23 corresponds to the nickel initial-uncorre-
lated density of states (N_e =9.4 el./bands) and Fig. 24 corresponds to
the bcc canonical d-band uncorrelated density of states /38/ with the
bandfilling appropriate for iron (N_e =7.4 el./bands). These results ob-
tained for realistic uncorrelated densities of states in a fully self-
consistent way confirm those of Bulk and Jelitto obtained within their
thermodynamically selfconsistent scheme. Namely, in a selfconsistent
approach there is except explicit dependence of the self-energy on the
Coulomb strength also additional pronounced implicit corrections. It is
interesting that with increasing correlation strength the self-energy

increases much slower than with U^2 factor. For that reason the results obtained within the selfconsistent approach even for greater values of the electron correlations could be more reliable than the corresponding non-selfconsistent results obtained for the same values of U.

In summary, we have compared the self-energy curves calculated within second-order U-perturbation treatment for the degenerate d-bands Hubbard model with full $\vec{k}$-dependence and within the local approximation. Based on this $\vec{k}$-dependent self-energy, we have calculated the spectral density of states, the quasiparticle energy bands and the quasiparticle density of states. Taking the $\vec{k}$-dependent self-energy one obtains narrower and sharper satellite structures on the quasiparticle energy bands. We have also compared all these results with those calculated in a self-consistent way. In this case, the spectral density of states has one-peaked character without any (besides the main peak) additional quasiparticle excitations present in a non-selfconsistent approach. As a consequence, also the quasiparticle density of states does not contain any satellite-like structures regardless of the correlation strength or band-filling.

References

1. C.S.Wang, J.Callaway, Phys.Rev. B15, 298 (1977).
2. S.Hüfner, G.K.Wertheim, N.V.Smith, M.M,Traum, Solid St. Comm. 11, 323 (1972).
3. F.J.Himpsel, J.A.Knapp, D.E.Eastman, Phys.Rev. B19, 2919 (1979).
4. C.Guillot, Y.Ballu, J.Paigne, J.Lecante, K.P.Jain, P.Thiry, R.Pinchaux, Y.Petroff, L.M.Falicov, Phys.Rev.Lett. 39, 1632 (1977).
5. Y.Sakisaki, T.Komeda, M.Ouchi, H.Kato, S.Masuda, K.Yagi, Phys.Rev. Lett. 58, 733 (1987).
6. D.E.Eastman, F.J.Himpsel, J.A.Knapp, Phys.Rev.Lett. 40, 1514 (1978).
7. E.Dietz, U.Gerhardt, C.Maetz, Phys.Rev.Lett. 40, 892, (1978).
8. W.Eberhardt, E.W.Plummer, Phys.Rev. B21, 3245 (1980).
9. J.Hubbard, Proc. Roy. Soc. A276, 238 (1963); A281, 401 (1964).
10. D.R.Penn, Phys.Rev.Lett. 42, 921 (1979).
11. A.Liebsch, Phys.Rev. B23, 5203 (1981); Fostkörperprobleme XIX, 209 (1979).
12. R.Victora, L.M.Falicov, Phys.Rev.Lett. 55, 1140 (1985).
13. J.Kanamori, Progr.Theor.Phys. 30, 275 (1963).

14. L.C.Davis, L.A.Feldkamp, Solid St.Comm. 34, 141 (1980); J.Appl.Phys. 50, 1944 (1979).

15. G.Treglia, F.Ducastelle, D.Spanjaard, J.Physique 41, 281 (1980); 43, 341 (1982).

16. A.M.Oleś, G.Treglia, D.Spanjaard, R.Jullien, Phys.Rev. B32, 2167 (1985); B34, 5101 (1986).

17. G.Bulk, R.J.Jelitto, Phys.Rev. B41, 413 (1990).

18. J.Friedel, C.M.Sayer, J.Physique 38, 697 (1977).

19. L.Kleinman, K.Mednick, Phys.Rev. B24, 6880 (1981).

20. N.I.Kulikov, M.Alouani, M.A.Khan, M.V.Magnitskaya, Phys.Rev. B36, 929 (1987).

21. R.Taranko, E.Taranko, Physica B153, 232 (1988).

22. R.Taranko, E.Taranko, J.Malek, J.Physics F18, L87 (1988).

23. R.Taranko, E.Taranko, J.Malek, J.Physics: Condensed Matter 1, 2935 (1989).

24. V.Zlatic, P.Entel, B.Horvatic, D.Schulz, Preprint ICTP/88/122, Miramare-Triest 1988.

25. H.Schweitzer, G.Czycholl, Solid St.Comm. 69, 171 (1989).

26. H.Schweitzer, G.Czycholl, Solid St.Comm., in print (1990).

27. H.Schweitzer, G.Czycholl, Z.Phys.B, 79, 377 (1990).

28. H.Schweitzer, G.Czycholl, Z.Phys. B, 74, 203 (1989).

29. G.Czycholl, Phys.Reports 141, 277 (1986).

30. R.Taranko, Preprint JINR E17-89-599, Dubna 1989.

31. T.Morita, T.Horiguchi, J.Math.Phys. 12, 986 (1971).

32. E.Taranko, R.Taranko, M.Piłat, Ann.Univ. M.Curie-Sklod. vol. XL/XL, sect. AAA, 1985/86, p. 489.

33. R.Taranko, E.Taranko, J.Malek, Preprint JINR E17-87-554, Dubna 1987.

34. C.Thuault, M.C.Desjonqueres, D.Spanjaard, J.Phys. C16, 5689 (1983). O.Bisi, C.Calandra, U. del Pennino, P.Sassoroli, S.Valeri. Phys.Rev. B30, 5696 (1984). C.Calandra, O.Bisi, Phys.Rev. B31, 8288 (1985).

35. W.Götze, "Diffusion and localisation of a particle in a two--dimensional random environment", Preprint TU München 1982.

36. K.I.Wysokinski, dissertation 1987 Lublin (not published). S.V.Vonsovskii, Yu.A.Izyumov, E.Z.Kurmaev, "Sverchprovodimost' perechodnych metallov, ich splavov i soedinienij", Nauka 1977, Moscov.

37. E.Müller-Hartmann, Z.Phys. B76, 211 (1989).

38. O.K.Andersen, O.Jepsen, D.Glötzel, in "Highlights of consensed Matter Theory", LXXXIX Corso Soc. Italiana di Fisica, Bologna,1985.